16 October 1998

ELSEVIER

Chemical Physics Letters 295 (1998) 298–304

CHEMICAL PHYSICS LETTERS

Two-dimensional THz spectroscopy of liquids: non-linear vibrational response to a series of THz laser pulses

Ko Okumura [1], Yoshitaka Tanimura

Institute for Molecular Science, Myodaiji, Okazaki, Aichi 444-8585, Japan

Received 27 July 1998; revised 17 August 1998

Abstract

We propose a non-linear experiment using the non-linear interaction with THz pulses, the generation of which has recently become well established. In the lowest non-linear process, we have two controllable delay times. This is another optical analogue of two-dimensional (2D) NMR as the recently developed 2D Raman spectroscopy. Our model calculation for liquid water demonstrates the striking capability of the proposed technique, clearly distinguishing two types of anharmonicity in the low-frequency modes. © 1998 Elsevier Science B.V. All rights reserved.

Many important phenomena such as chemical reactions and protein folding usually occur only in solution. In such cases, liquid dynamics certainly plays an indispensable role. Understanding of these phenomena should be based upon a proper knowledge of liquid.

Recent progress in the ultrafast pulse laser technique has contributed greatly to this understanding. It allows us to probe liquid dynamics in the timescale of chemical reactions [1–4]. For example, third-order off-resonant spectroscopy, such as the femtosecond optical Kerr effect, has revealed valuable information on vibrational motion of liquids. It has also been found that some properties such as inhomogeneity and anharmonicity cannot be investigated intrinsically in third-order experiments. This recognition has led currently to the explosive development in the field of highly non-linear spectroscopy, such as two-dimensional (2D) Raman spectroscopy [5–14], which uses the fifth-order off-resonant process.

The 2D Raman spectroscopy was initially proposed [5] to distinguish inhomogeneity from homogeneity in liquids. Recent study revealed that this spectroscopy is also capable of detecting anharmonicity in the coordinate dependence of vibrational potential and non-linearity in that of polarizability, even though they are weak [10]. Currently, it is also understood that it can be a valuable tool in studying the coupling mechanism between or within the vibrational modes [11,12,14].

The femtosecond laser technique has also made it possible to generate THz laser pulses that opened new fields from THz time-resolved spectroscopy to so-called T-ray imaging. The excitation of charge carriers in a

[1] Corresponding author. E-mail: okumura@ims.ac.jp

0009-2614/98/$ - see front matter © 1998 Elsevier Science B.V. All rights reserved.
PII: S0009-2614(98)00968-3

semiconductor material with the femtosecond pulses generates the THz pulses [15] which are nearly a single cycle and covers the THz frequency range (see Fig. 1).

A variety of techniques can be used to measure the vibrational spectrum in this low-frequency range (1–100 cm^{-1}). Among these are FT-FIR spectroscopy, Raman scattering, and the above-mentioned off-resonant techniques. The relatively new THz laser pulse is also promising as a probe for low-frequency vibrational dynamics. The THz pulse can excite and probe the low-frequency modes of liquids directly (not through the Raman process), and the detection technique allows us to obtain the signal (complex) amplitude instead of intensity.

Accordingly, the new source has been actively used to investigate the low-frequency modes of liquids [16–21], providing us with a new insight. These cases include the non-linear experiment using a visible pump followed by a THz probe; the observed process involves the interaction of the THz pulse with the sample only once.

We shall discuss possible experiments using more than two THz pulses; we investigate the possibility of a THz analogue of 2D Raman spectroscopy. In 2D Raman spectroscopy, availability of the two controllable delay times is essential. Thus, we use more than two THz pulses to excite the sample more than twice and observe the generated signal. There are several essential differences between this resonant spectroscopy and the (off-resonant) 2D Raman spectroscopy.

Firstly, we observe the correlation of dipole moment instead of polarizability; the selection rules are different and both are thus complementary to each other.

Secondly, we observe the n-time correlation function as the $(n-1)$th order signal instead of the $(2n-1)$th order. For example, a three-time correlation function of the dipole moment $R_{\mu}^{(3)} = \langle [[\mu(t), \mu(t')], \mu(0)] \rangle$ is observed in second-order THz spectroscopy while that of the polarizability $R_{\alpha}^{(3)} = \langle [[\alpha(t), \alpha(t')], \alpha(0)] \rangle$ is measured in fifth-order off-resonant spectroscopy. This implies that the $2n$th-order THz signal is zero in isotropic liquids or a system with inversion symmetry, since it is a $\chi^{(2n)}$ process. The lowest non-linear process is the third order in the THz field and corresponds to the four-time correlation function.

Thirdly, the pulse duration is comparable to the nuclear dynamics while, in the femtosecond off-resonant case, it can be treated as the delta function for nuclear dynamics. This makes analysis of the THz case difficult; we have to perform one time integral per each THz pulse interaction. However, the difficulty is a tractable one; we shall demonstrate that the calculated non-linear THz signal shows a significant capability in distinguishing various microscopic origins.

Finally, it is more appropriate to regard the THz pulse as a superposition of many plane waves with a wide frequency range rather than a multiple of an envelope function and a single plane wave.

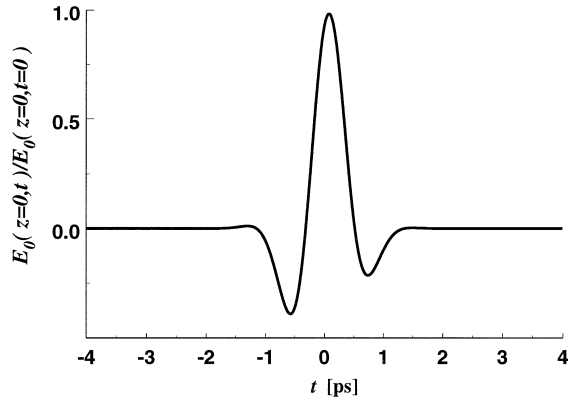

Fig. 1. The THz pulse shape, $E_0(z=0,t)$, employed in the calculation. The Fourier transform of the profile, $E_0(\omega)$, has a finite amplitude in the frequency range from -60 to 60 cm^{-1}.

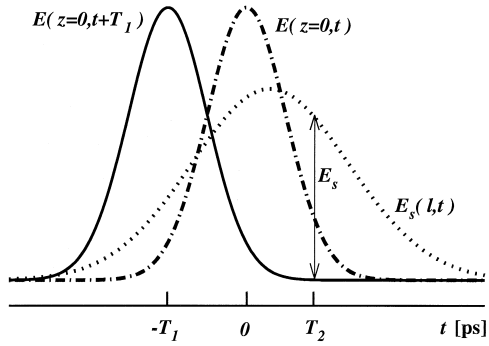

Fig. 2. The pulse configuration of the proposed experiment. The lines stand for the envelopes of the THz signals. The first pulse, $E(z=0,t+T_1)$, is followed by the second one, $E(z=0,t)$, after time T_1. The generated signal $E_s(l,t)$ is then observed after time T_2 from the second input pulse: $E_s \equiv E_s(l,T_2)$.

To clarify our points, we consider two THz pulses moving in the z-direction, where the sample occupies the space $0<z<l$. The polarization of both fields is assumed to be perpendicular to the moving direction z, say in the x direction. The time delay of the two pulses is denoted T_1. We then observe the signal which is polarized in the x direction after time T_2 from the second input. Thus, we have the two controllable times T_1 and T_2 (see Fig. 2).

A THz pulse which peaks at time $t=0$ at position $z=0$ can generally be expressed as

$$E_0(z,t)=\int_{-\infty}^{\infty} \mathrm{d}\omega\, E_0(\omega)\mathrm{e}^{\mathrm{i}kz-\mathrm{i}\omega t}, \tag{1}$$

where the wave number is given by $k=\omega/c$ and $E_0(\omega)$ is determined by $E_0(z=0,t)=\int \mathrm{d}\omega \mathrm{e}^{-\mathrm{i}\omega t}E_0(\omega)$.

We define the time zero as the time when the second pulse arrives at $z=0$. The field in the medium $(0<z<l)$ can be expressed as

$$E_T(z,t)=E(z,t+T_1)+E(z,t), \tag{2}$$

where

$$E(z,t)=\int_{-\infty}^{\infty} \mathrm{d}\omega\, E_r(\omega)\,\mathrm{e}^{\mathrm{i}k_r(\omega)z-\mathrm{i}\omega t}. \tag{3}$$

Here, $E_r(\omega)\mathrm{e}^{\mathrm{i}k_r(\omega)z-\mathrm{i}\omega t}$ is continued from the plane wave in the atmosphere, $E(\omega)\mathrm{e}^{\mathrm{i}kz-\mathrm{i}\omega t}$, at the vacuum-medium boundary $(z=0)$. By the Fresnel law, the transmission amplitude $E_r(\omega)$ is given by $E_r(\omega)=2E_0(\omega)/(1+\sqrt{\epsilon(\omega)})$. By Snell's law, the complex wave number $k_r(\omega)$ is given by $\omega\sqrt{\epsilon(\omega)}/c$, where $\epsilon(\omega)$ is the complex dielectric constant, or

$$k_r(\omega)=k_r'(\omega)+\mathrm{i}|\alpha(\omega)|/2. \tag{4}$$

The real wave number $k_r'(\omega)$ and the absorption coefficient $\alpha(\omega)$ are, respectively, given as the real and imaginary parts of the complex dielectric constant $\epsilon(\omega)$ ($|\cdots|$ stands for the absolute value).

The macroscopic polarization induced in the medium can be expressed as

$$P(z,t)=P^{(0)}+P^{(1)}(z,t)+P^{(2)}(z,t)+\cdots, \tag{5}$$

where $P^{(0)}$ is the permanent polarization and $P^{(i)}(z,t)$ is the ith-order induced polarization. For example, the third-order induced polarization is given by [22]

$$P^{(3)}(z,t) = \int_{-\infty}^{\infty} \mathrm{d}t_1 \int_{-\infty}^{\infty} \mathrm{d}t_2 \int_{-\infty}^{\infty} \mathrm{d}t_3\, R(t_1,t_2,t_3)\, E_T(t-t_3)\, E_T(t-t_3-t_2)\, E_T(t-t_3-t_2-t_1)\,, \tag{6}$$

where

$$R(t_1,t_2,t_3) = \theta(t_1)\theta(t_2)\theta(t_3)\rho(i/\hbar)^3 \langle [[[\mu(t_1+t_2+t_3),\mu(t_1+t_2)],\mu(t_1)],\mu(0)]\rangle\,, \tag{7}$$

and ρ is the density of dipole moment. Since $P^{(1)}(z,t)$ can be included in $\epsilon(\omega)$ below and $P^{(2)}(z,t)$ vanishes for an isotropic medium, the generated field $E_s(z,t)$ may be determined by the equation,

$$\frac{\partial^2 E_s(z,\omega)}{\partial z^2} + \frac{\omega^2}{c^2}\epsilon(\omega) E_s(z,\omega) = -\frac{\omega^2}{c^2\epsilon_0} P^{(3)}(z,\omega), \tag{8}$$

where $E_s(z,\omega)$ and $P^{(3)}(z,\omega)$ are the Fourier components. The signal is then given a function of the delay time T_2: $E_s \equiv E_s(l,T_2)$.

A general solution of Eq. (8) can be expressed as

$$E_s(z,\omega) = c_1\, \mathrm{e}^{\mathrm{i}k_r(\omega)z} + c_2 \mathrm{e}^{-\mathrm{i}k_r(\omega)z} - \frac{\omega^2}{2\mathrm{i}k_r(\omega)c^2\epsilon_0}\left\{\int_0^z \mathrm{d}z'\, \mathrm{e}^{\mathrm{i}k_r(\omega)(z-z')} P^{(3)}(z',\omega) + \int_z^l \mathrm{d}z'\, \mathrm{e}^{-\mathrm{i}k_r(\omega)(z-z')} P^{(3)}(z',\omega)\right\}. \tag{9}$$

where c_1 and c_2 are constants. Since $E_s(z,\omega)$ should be zero when $P^{(3)}(z,\omega)$ is zero for $0<z<l$, we obtain $c_1 = c_2 = 0$. Thus, at $z=l$, $E_s(z,\omega)$ formally coincides with the one obtained by the slowly-varying envelope approximation. When one compares the calculated signal with the experiment, one should note that the signals presented in this Letter are the signal generated at the inside of the medium boundary, $z=l$.

We have calculated the signals, E_s, for a Brownian oscillator model, which has been used to analyze the 2D Raman experiments [5,6,8–12], and the salient features of our results will be shown below. We consider the case where the low-frequency responses are described by s representative modes, $Q_1,\ldots,Q_s$. The potential of the system is expressed as

$$V(Q) = \sum_{i=1}^{s} \frac{M_i}{2}\Omega_i^2 Q_i^2 + \sum_{i,j,k} \frac{g_{i,j,k}}{3!} Q_i Q_j Q_k + \cdots\,. \tag{10}$$

The dipole moment is also expanded by the coordinates:

$$\mu(Q) = \mu_0 + \sum_{i=1}^{s} \mu_i Q_i + \sum_{i,j} \frac{\mu_{i,j}}{2!} Q_i Q_j + \cdots\,. \tag{11}$$

From a simple argument [23], we can show that the signal E_s vanishes if both the anharmonicity and the non-linearity are zero. Thus, this signal is sensitive to the weak anharmonicity and weak non-linearity.

As an example, we study liquid water with the sample thickness $l = 100\ \mu$m. We employed the Brownian oscillator model characterized by the spectral distribution,

$$J(\omega) = \sum_i \frac{\omega\eta_i\gamma_i}{\left(\omega_i^2-\omega^2\right)^2 + \omega^2\gamma_i^2}\,. \tag{12}$$

We found that the recent dielectric measurements [16] can be fit by the two damped oscillators with $(\omega_{\mathrm{L}},\gamma_{\mathrm{L}},\sqrt{\eta_{\mathrm{L}}}) = (10,100,70.7)$ and $(\omega_{\mathrm{H}},\gamma_{\mathrm{H}},\sqrt{\eta_{\mathrm{H}}}) = (200,250,387)$ (in the unit cm^{-1}).

For simplicity, we assume that the dipole moment is linear, i.e. $\mu_{i,j} = \cdots = 0$, and there are no couplings between the modes, i.e. $g_{i_1,i_2,\ldots,i_n} = 0$, unless $i_1 = i_2 = \cdots = i_n$, where $g_{i_1,i_2,\ldots,i_n}$ is the coefficient of the nth order anharmonicity. Then, the signal is composed of the terms proportional to the normalized anharmonicity $\bar{g}_i$, which is proportional to the coefficient of the fourth-order anharmonicity, $g_{i,j,k,l}$. Apart from the prefactor $\bar{g}_i$, all the parameters can be determined by the dielectric data as shown above. This spectroscopy has the potential to determine the relative importance of the (normalized) anharmonicity.

Note here that only the relative strength of the signals can be compared in our calculation. This is because the signal is proportional to the prefactor $\bar{g}_i$, which can be expressed by unknown parameters and a little change in them can cause a large difference in $\bar{g}_i$.

We depict the 2D signals for (1) an anharmonic low-frequency mode ($\bar{g}_{\mathrm{L}} \neq 0, \bar{g}_{\mathrm{H}} = 0$) and (2) an anharmonic high-frequency mode ($\bar{g}_{\mathrm{L}} = 0, \bar{g}_{\mathrm{H}} \neq 0$) in Figs. 3 and 4, respectively.

At $T_1 = 0$ the two equivalent THz pulses are superposed. This can be considered as a single THz pulse with a double amplitude (see Eq. (2)). The T_2-time development monitors merely the relaxation of the system after the *single* excitation. However, the observed process is non-linear in which the single pulse interacts with the sample three times (see Eq. (6)). As seen in Figs. 3 and 4 the profiles in the two cases are quite different. We also checked that the decay time in case (1) is much longer than the other.

If T_1 is large, the second pulse arrives after the excitation created by the first THz pulse is relaxed completely. Then, the overall decay processes are divided into two components separated by T_2, each of which has the same profile with that at $T_1 = 0$. Note that the amplitude of each component should be one-eighth of the amplitude at $T_1 = 0$, since the pulse amplitude is doubled in the case of $T_1 = 0$ and the signal is proportional to E_0^3. In case (2), at $T_1 = 2$ (ps), we see that the whole profile is well separated into two components. Each profile has nearly the same profile of the signal at $T_1 = 0$ with the one-eighth amplitude. On the contrary, in case (1),

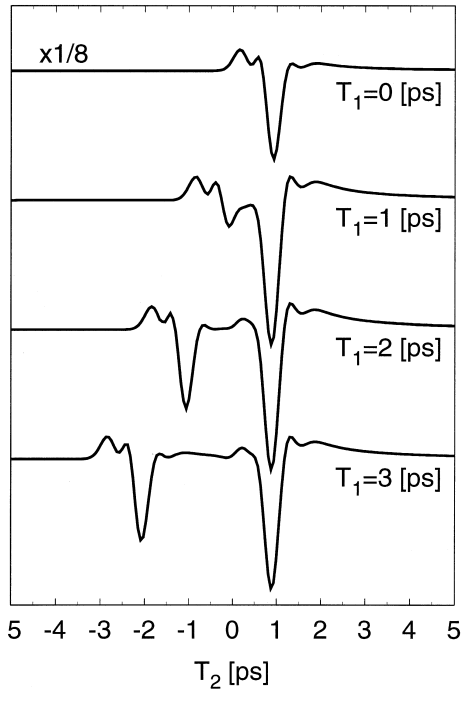

Fig. 3. Case (1): The calculated signal in the case where the low-frequency mode (ω_{L}) has the anharmonicity. The signals are plotted in the same arbitrary unit except for the top one. The amplitude of the plot at $T_1 = 0$ is one-eighth of the actual one as indicated in the figure. See the text for details.

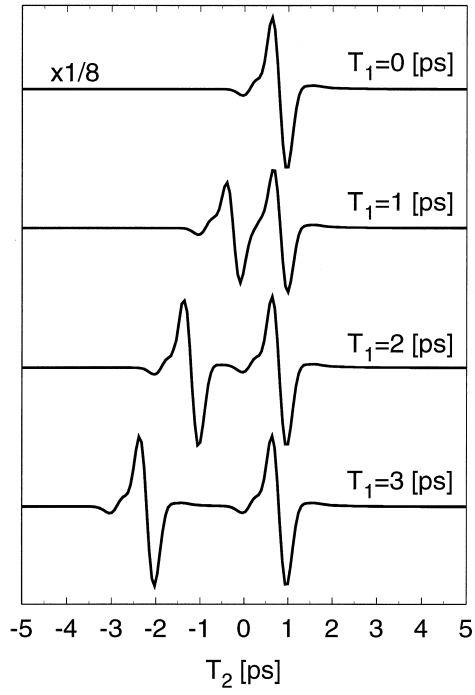

Fig. 4. Case (2): The calculated signal in the case where the high-frequency mode (ω_H) has the anharmonicity.

the two components do not look independent even at $T_1 = 3$ (ps). We checked that each of them becomes exactly one-eighth of the profile at $T_1 = 0$ only after $T_1 = 15$ (ps). This difference reflects the above-mentioned large difference in the decay times.

In the region where T_1 lies between the above two limiting regimes, the two components look as if they are interacting with each other.

As a whole, there is a marked difference between cases (1) and (2). This suggests a possibility that one can investigate the interplay of the two anharmonic contributions from experiment.

In this Letter, we assumed that the sample has any non-linearity in the dipole moments as a demonstration. However, it is easy to take into account the non-linearity of the dipole moments. We also assumed the collinear geometry for the input THz pulses in the above. This implies that a weak third-order signal is superposed on the original input pulses. This can be difficult to detect although the THz detection technique currently allows a relatively high signal-to-noise ratio. In such case, it would be better to detect the generated signal in a direction different from those of the original inputs. The study for this situation will be published elsewhere.

This technique should not be limited to liquids and it can also be applied to solids. In the case where the sample lacks the inversion symmetry, the source term in Eq. (8) becomes $P^{(2)}$ instead of $P^{(3)}$. This case is also under study.

In conclusion, we have demonstrated that the proposed non-linear THz pulse spectroscopy has a great potential just like 2D Raman spectroscopy. However, the information obtained in the two spectroscopic techniques complements each other. As an example, we showed that the proposed experiment could clearly distinguish the microscopic information on the low-frequency modes of liquids. As in 2D Raman spectroscopy, this non-linear technique also allows distinction between inhomogeneity and homogeneity, which is intrinsically impossible in the lower-order experiment. In addition, 2D Fourier transformation may give another insight into the low-frequency modes as well. These are also important issues which require separate study.

Acknowledgements

We would like to thank Koichi Shimoda and Charles Schmuttenmaer for fruitful discussions. The present work was supported by a Grant-in-Aid for Scientific Research from the Japan Ministry of Education, Science, Sports, and Culture.

References

[1] M. Cho, M. Du, N.F. Scherer, G.R. Fleming, J. Chem. Phys. 99 (1993) 2410.
[2] L. Dhar, J.A. Rogers, K.A. Nelson, Chem. Rev. 94 (1994) 157.
[3] D. McMorrow, N. Thantu, J.S. Melinger, S.K. Kim, W.T. Lotshaw, J. Chem. Phys. 100 (1996) 10389.
[4] K.D. Rector, M.D. Fayer, J. Chem. Phys. 108 (1998) 1974.
[5] Y. Tanimura, S. Mukamel, J. Chem. Phys. 99 (1993) 9496.
[6] K. Tominaga, K. Yoshihara, Phys. Rev. Lett. 74 (1995) 3061.
[7] K. Tominaga, Advances in Multi-Photon Processes and Spectroscopy, vol. 11, World Scientific, Singapore, in press.
[8] T. Steffen, K. Duppen, Phys. Rev. Lett. 76 (1996) 1224.
[9] A. Tokmakoff, G.R. Fleming, J. Chem. Phys. 106 (1997) 2569.
[10] K. Okumura, Y. Tanimura, J. Chem. Phys. 107 (1997) 2267.
[11] A. Tokmakoff, M.J. Lang, D.S. Larsen, G.R. Fleming, V. Chernyak, S. Mukamel, Phys. Rev. Lett. 79 (1997) 2702.
[12] K. Okumura, Y. Tanimura, Chem. Phys. Lett. 277 (1997) 159.
[13] R.L. Murry, J.T. Fourkas, J. Chem. Phys. 107 (1997) 9726.
[14] S. Saito, I. Ohmine, J. Chem. Phys. 108 (1998) 240.
[15] D.H. Auston, K.P. Cheung, J.A. Valdmanis, D.A. Kleinman, Phys. Rev. Lett. 53 (1984) 1555.
[16] J.T. Kindt, C.A. Schmuttenmaer, J. Phys. Chem. 100 (1996) 10373.
[17] B.N. Flanders, R.A. Cheville, D. Grischkowsky, N.F. Scherer, J. Phys. Chem. 100 (1996) 11824.
[18] D.M. Mittleman, M.C. Nuss, V.L. Colvin, Chem. Phys. Lett. 275 (1997) 332.
[19] G. Haran, W.-D. Sun, K. Wynne, R.M. Hochstrasser, Chem. Phys. Lett. 274 (1997) 365.
[20] R. McElroy, K. Wynne, Phys. Rev. Lett. 79 (1997) 3078.
[21] E.J. Heilweil, private communication.
[22] S. Mukamel, Principle of Nonlinear Optical Spectroscopy, Oxford, New York, 1995.
[23] K. Okumura, Y. Tanimura, J. Chem. Phys. 106 (1997) 1687.